



## Bifurcation Analysis of a Mathematical Model for the Covid-19 Infection among Pregnant and Non-Pregnant Women

Jonathan Tsetimi<sup>1,\*</sup>, Marcus Ifeanyi Ossaiugbo<sup>1</sup>, Augustine Atonuje<sup>1</sup>

<sup>1</sup> *Department of Mathematics, Delta State University, Abraka, Delta State, Nigeria*

---

**Abstract.** A mathematical study and analysis of the covid-19 disease is essential in the control and eradication of the dreadful covid-19 infection. This research work is focused on the covid-19 infection among the women population. The women population was divided into seven compartments. These compartments were built into a deterministic model presented as a system of ordinary differential equations. Basic mathematical analyses such as positivity of solution, the disease-free equilibrium and the basic reproduction number, were performed on the model. The model assumes only positive solutions and the total population size is bounded. The next generation matrix approach was employed in generating the basic reproduction number  $R_0$ . The sensitivity analysis revealed that among the most sensitive parameters of  $R_0$  are the effective contact rate for covid-19 transmission, the modification parameter accounting for increased susceptibility to covid-19 infection by pregnant women, and the transmission coefficient of the infectious pregnant women. The bifurcation analysis revealed a forward bifurcation which guarantees the stability of the disease-free equilibrium when  $R_0$  is lowered below unity. Numerical simulations, using Mathematica Version 12.0 package, are given to show the effects of the most sensitive parameters of the basic reproduction number on the number of infectious cases of covid-19.

**2020 Mathematics Subject Classifications:** 34A34, 37D99, 37G99, 03C99

**Key Words and Phrases:** Covid-19, Bifurcation, Sensitivity, Simulation, Mathematical model

---

### 1. Introduction

Maternal health is affected both directly and indirectly by the Covid-19 pandemic, and pregnant individuals were found to be at a heightened risk of more severe symptoms than people who are not pregnant [9]. Studies have suggested that pregnant women are more susceptible to COVID-19 compared to non-pregnant women [10]. [11] also revealed that

---

\*Corresponding author.

DOI: <https://doi.org/10.29020/nybg.ejpam.v15i2.4312>

*Email addresses:* [jtsetimi@delsu.edu.ng](mailto:jtsetimi@delsu.edu.ng); [tsetimi@yahoo.com](mailto:tsetimi@yahoo.com) (J. Tsetimi),  
[iossaiugbo@delsu.edu.ng](mailto:iossaiugbo@delsu.edu.ng); [marcusossaiugbo@gmail.com](mailto:marcusossaiugbo@gmail.com) (M. I. Ossaiugbo),  
[atonuje@delsu.edu.ng](mailto:atonuje@delsu.edu.ng) (A. Atonuje)

COVID-19 may predispose pregnant women to higher risks of severe disease and poorer neonatal outcome. They also highlighted the importance of appropriate counselling by clinicians, and focused clarification on the effect of COVID-19 among pregnant women to be made for mental wellbeing and psychological support of pregnant women. [6] added that in unvaccinated pregnant women, Covid-19 can cause deadly harm to babies as the disease can attack and destroy the placenta. [10] suggested that education of pregnant women on COVID-19 preventive practices should be intensified at health facilities while improving upon the water, sanitation and hygiene need particularly in rural communities. The severity of the COVID-19 disease is significantly associated with increased cesarean delivery, admission to the intensive care unit, and cases of maternal mortality [18].

Mathematical modeling of infectious diseases has proven to be an effective tool in the management, control and eradication of infectious diseases. A mathematical model of an infectious disease gives clear dynamics of the disease. The relationship between the variables and parameters involved in the dynamics of an infectious disease are clearly stated in its mathematical model, and are often supported by a schematic diagram. Different mathematical models exist for various infectious diseases and these models often study various aspects of the diseases. Some of the models which exist in literature for the covid-19 infectious disease include [1, 4, 15]. [4] estimated the effective reproduction number of COVID-19 from the next generation in the presence of intervention and opined that collaborated efforts from individual, media and integrated government interventions were the only way to reduce the effective reproduction number to a figure below 1. They added that individuals must adhere to the prevention protocols and the media must intensify its daily report on COVID-19 cases to improve behavioral change, which have beneficial impact on the incidence cases.

[1] proposed a system of five non-linear ordinary differential equations to study the COVID-19 infection and mathematical analysis of the model were carried out, where boundedness, computation of equilibria, calculation of the basic reproduction ratio and stability analysis of the equilibria were carried out. [15] showed the suitability of proposed COVID-19 model for the outbreak that occurred in Wuhan, China. The model divides the entire population into eight compartments. By the parameter values used in their research, they obtained the basic reproduction number as  $R_0 = 0.945$ .

[23] implemented an attractive reliable analytical technique for constructing numerical solutions for the fractional Lienard's model enclosed with suitable nonhomogeneous initial conditions, which are often designed to demonstrate the behavior of weakly nonlinear waves arising in the oscillating circuits. [24] proposed the Atangana–Baleanu fractional methodology for fathoming the Van der Pol damping model by using the reproducing kernel algorithm.

In this research work, we shall be considering the bifurcation and sensitivity analyses of a deterministic model for the covid-19 infection among pregnant and non-pregnant women. The effects of the effective contact rate, delivery rate, transmission coefficient of the class of infectious pregnant women and modification parameter accounting for increased susceptibility to covid-19 infection by pregnant women over the population of infectious individuals shall also be considered.

## 2. Model Description and Formulation

In the model, we let  $S_p(t)$  denote the total number of pregnant women who are susceptible to the covid-19 infection at time  $t$ , while  $S_n(t)$  represents the population of non-pregnant women who are susceptible to the covid-19 infection at time  $t$ . The total number of pregnant women who are infectious of the covid-19 disease at time  $t$  is represented by  $I_p(t)$ , while the population of non-pregnant women at time  $t$  is represented by  $I_n(t)$ .  $H(t)$  denotes the population of women who are both infectious of the disease and are hospitalised at time  $t$ . We let the total number of pregnant women who have recovered from the disease at time  $t$  be represented by  $R_p(t)$  and the total population of non-pregnant women at time  $t$  be represented by  $R_n(t)$ .

The model divides the total women population into compartments namely  $S_n, I_n, R_n, H, S_p, I_p, R_p$ . The total population is given as

$$N(t) = S_n(t) + I_n(t) + R_n(t) + H(t) + S_p(t) + I_p(t) + R_p(t). \quad (1)$$

The model is based on the following assumptions:

1. Both infectious expectant and infectious non-expectant mothers are kept in the same health care facility.
2. Disease-induced death rate is same for both pregnant and non-pregnant women.
3. The conception rate is the same for the susceptible, infectious and recovered compartments.
4. The delivery rate is the same for the susceptible, infectious and recovered compartments.

### The susceptible class for non-pregnant women

Non-pregnant women are recruited into the susceptible class  $S_n$  at the rate  $\Lambda$ . This class is also increased by women from the class  $S_p$  who have been delivered of their babies at the rate  $\theta$ . Non-pregnant women who have recovered from the covid-19 disease can become susceptible to the disease at the rate  $\Psi$ . Women leave this compartment when they become infected at the rate  $\chi$  and they join the infectious class  $I_n$  for the non-pregnant women. The rate  $\chi$  is frequency of occurrence of new instances of the covid-19 infection within the given population under consideration during a specific period of time. This parameter is very important in this model since it is directly proportional to the average number of infections.  $\chi$  is the force of infection of the covid-19 disease and it is defined as  $\chi = k(1 - \varpi) \frac{I_n + \rho I_p + \iota H}{N}$  where  $k$  is the effective contact rate for covid-19 transmission,  $\varpi$  is the rate of adherence of women to government's regulations on vaccination, social distancing, hand-washing and the use of nose mask and sanitizer. A high value of  $k$  means an increased force of infection and this can boost the number of infectious cases of

the covid-19 disease among the women population.  $\varrho$  and  $\iota$  are transmission coefficients for the pregnant infectious women and the hospitalised women respectively. The value of  $\iota$  is expected to be relatively small compared to the value of  $\varrho$  since the women in the hospitalised compartment are constrained to follow strict preventive measures and possible isolation, hence their transmission coefficient must be relatively low. Women who become pregnant also leave this compartment and are joined to the susceptible class ( $S_p$ ) for pregnant women. The population of this class  $S_n$  is also reduced by natural death at the rate  $\mu$ . Thus, the equation for this class is given as

$$\frac{dS_n}{dt} = \Lambda + \theta S_p + \Psi R_n - (\delta + \mu + \chi)S_n. \quad (2)$$

### The infectious class for non-pregnant women

The infectious class  $I_n$  of non-pregnant women is increased by non-pregnant women who have caught the covid-19 disease by the force of infection  $\chi$  and are now infectious. Infectious pregnant women who have been delivered of their babies also join this class at the rate  $\theta$ . Women in this class conceive at the rate  $\delta$  and move into the infectious class for pregnant women. Non-pregnant infectious women are hospitalised/quarantined at the rate  $\varepsilon$ . The recovery rate of women in this infectious class  $I_p$  is  $\eta$ . The higher the value of  $\eta$ , the faster the elimination of the covid-19 infection from the pregnant women population. The size of this class is also reduced by disease-induced deaths at the rate  $\varsigma$ . Natural death also occurs in this infectious class at the rate  $\mu$ . The equation for the compartment is given as

$$\frac{dI_n}{dt} = \chi S_n + \theta I_p - (\delta + \varepsilon + \eta + \mu + \varsigma)I_n. \quad (3)$$

### The recovered class for non-pregnant women

Individuals from the infectious class  $I_n$  and the hospitalised class  $H$  join the recovered class  $R_n$  at the rates  $\eta$  and  $p\varphi$  respectively, where  $p$  is the proportion of hospitalised individuals who have recovered from the disease but are not pregnant. Pregnant women in the class  $R_p$  who have recovered from the disease and have been delivered of their babies are also added to this class  $R_n$ . As a result of loss of immunity, individuals in this compartment return to the class  $S_n$  at the rate  $\Psi$ . Individuals also leave this class for the class  $R_p$  due to conception at the rate  $\delta$ . Natural death occurs here at the rate  $\mu$ .

$$\frac{dR_n}{dt} = \theta R_p + p\varphi H + \eta I_n - (\delta + \mu + \Psi)R_n. \quad (4)$$

### The hospitalised class

The population of this class is increased by individuals from the compartments  $I_n$  and  $I_p$ . Individuals in the infectious classes  $I_n$  and  $I_p$  are hospitalised at the rates  $\varepsilon$  and  $\alpha$  respectively. The recovery rate of these women who have been hospitalised is  $\varphi$ , while

disease-induced death also occurs in this class at the rate  $\varsigma$ . Individuals in this class can also die due to natural death at the rate  $\mu$ .

$$\frac{dH}{dt} = \varepsilon I_n + \alpha I_p - (\mu + \varsigma + \varphi)H. \tag{5}$$

### The susceptible class for pregnant women

The recruitment rate of pregnant women into the susceptible class  $S_p$  is denoted by  $\Pi$ . This compartment is also increased by pregnant women who have recovered from the disease but lost their immunity. This women return to the susceptible class at the rate  $\sigma$ . Individuals in the class  $S_n$  move into the class  $S_p$  due to conception at the rate  $\delta$ . Individuals in this compartment can become infected at the rate  $\beta\chi$  and join the infectious class  $I_p$  where  $\beta$  is the modification parameter accounting for increased susceptibility to covid-19 infection by pregnant women. This modification parameter of the force of infection is very important when considering the dynamics of the covid-19 infection among pregnant women. It is expected that  $\beta$  raises the value of the force of infection for the pregnant women. Women in this compartment can also move into the class  $S_n$  due to delivery at the rate  $\theta$ . Natural death also occurs in this class at the rate  $\mu$ .

$$\frac{dS_p}{dt} = \Pi + \delta S_n + \sigma R_p - (\beta\chi + \theta + \mu)S_p. \tag{6}$$

### The infectious class for pregnant women

The population of individuals in this class  $I_p$  is increased by individuals from the classes  $S_p$  and  $I_n$  at the rates  $\beta\chi$  and  $\delta$  respectively. Individuals in this class are hospitalised at the rate  $\alpha$ . Infectious individuals who have been delivered of their babies leave this class and join the class  $I_n$  at the rate  $\theta$ . The recovery rate of infectious pregnant women is  $\gamma$ . Pregnant women in this compartment die due to the disease and also due to natural death at the rates  $\varsigma$  and  $\mu$  respectively. The severity of the covid-19 infection among pregnant women directly influences the value of  $\varsigma$ .

$$\frac{dI_p}{dt} = \delta I_n + \beta\chi S_p - (\alpha + \gamma + \theta + \mu + \varsigma)I_p. \tag{7}$$

### Recovered class for pregnant women

This class is increased by individuals from the classes  $H$ ,  $R_n$  and  $I_p$  at the rates  $(1-p)\varphi$ ,  $\delta$  and  $\gamma$  respectively, where the parameters have been defined earlier and are clearly stated in table 1. Individuals in this class who have been delivered of their babies join the class  $R_n$  at the rate  $\theta$ . Recovered pregnant women can return to the susceptible class  $S_p$  at the rate  $\sigma$ , due to loss of immunity. Natural death also occurs in this compartment at the rate  $\mu$ .

$$\frac{dR_p}{dt} = (1 - p)\varphi H + \delta R_n + \gamma I_p - (\theta + \mu + \sigma)R_p. \tag{8}$$

Thus the mathematical model is given as:

$$\begin{cases} \frac{dS_n}{dt} = \Lambda + \theta S_p + \Psi R_n - (\delta + \mu + \chi)S_n \\ \frac{dI_n}{dt} = \chi S_n + \theta I_p - (\delta + \varepsilon + \eta + \mu + \varsigma)I_n \\ \frac{dR_n}{dt} = \eta I_n + \theta R_p + p\varphi H - (\delta + \mu + \Psi)R_n \\ \frac{dH}{dt} = \varepsilon I_n + \alpha I_p - (\mu + \varsigma + \varphi)H \\ \frac{dS_p}{dt} = \Pi + \delta S_n + \sigma R_p - (\beta\chi + \theta + \mu)S_p \\ \frac{dI_p}{dt} = \beta\chi S_p + \delta I_n - (\alpha + \gamma + \theta + \mu + \varsigma)I_p \\ \frac{dR_p}{dt} = (1-p)\varphi H + \delta R_n + \gamma I_p - (\theta + \mu + \sigma)R_p \\ \chi = k(1 - \varpi) \frac{I_n + \varrho I_p + \iota H}{N} \\ N(t) = S_n(t) + I_n(t) + R_n(t) + H(t) + S_p(t) + I_p(t) + R_p(t) \end{cases} \quad (9)$$

The schematic diagram is shown in figure 1, while the description of state variables and parameters are given in table 1.

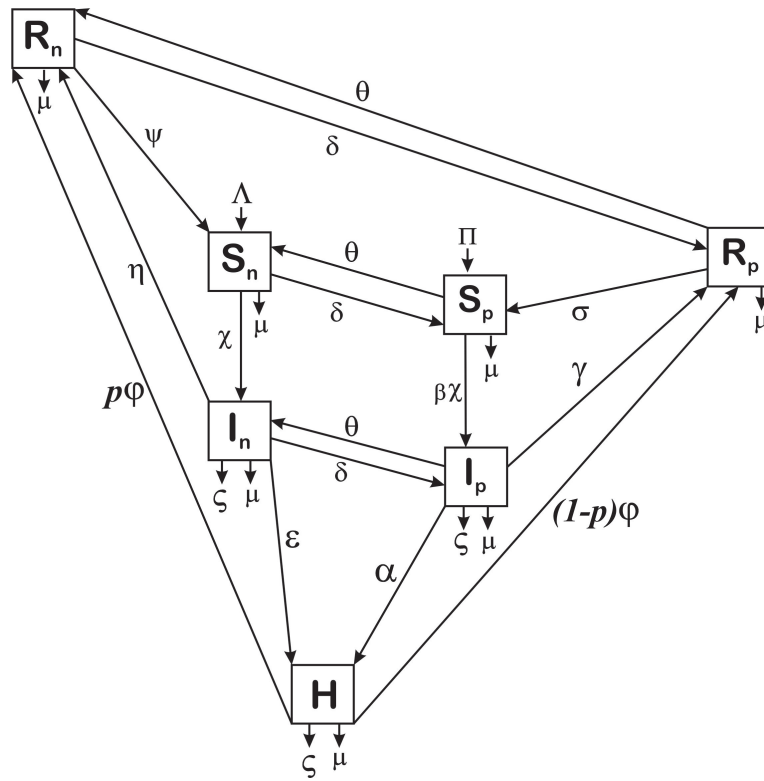


Figure 1: Schematic Diagram

Table 1: Variables and Parameters Description

<b>Variables/ Parameters</b>	<b>Descriptions</b>
$S_n$	Susceptible class for non-pregnant women
$I_n$	Infectious class for non-pregnant women
$R_n$	Recovered class for non-pregnant women
$H$	Class of hospitalised individuals
$S_P$	Class of susceptible pregnant women
$I_P$	Class of infectious pregnant women
$R_P$	Class of recovered pregnant women
$\Lambda$	Recruitment rate into the susceptible class for non-pregnant women
$\Pi$	Recruitment rate into the susceptible class for pregnant women
$\chi$	Force of infection
$\kappa$	Effective contact rate for covid-19 transmission
$\varpi$	Rate of adherence of individuals to government’s regulations like the compulsory wearing of good nose masks, washing of hands, social distancing, etc.
$\beta$	Modification parameter accounting for increased susceptibility to covid-19 infection by pregnant women
$\mu$	Natural death rate
$\varsigma$	Disease-induced death rate
$\varepsilon$	Rate at which infectious non-pregnant women move into the hospitalised class
$\alpha$	Rate at which infectious pregnant women move into the class of hospitalised individuals
$\eta$	Recovery rate of non-pregnant infectious individuals
$\gamma$	Recovery rate of infectious pregnant women
$\varphi$	Recovery rate of hospitalised individuals
$p$	Proportion of hospitalised individuals who recover from the disease but are not pregnant
$\Psi$	Rate at which recovered non-pregnant women become susceptible
$\sigma$	Rate at which pregnant women who have recovered from the covid-19 infection move into the susceptible class
$\delta$	Conception rate
$\theta$	Delivery rate
$\iota$	Transmission coefficient of the hospitalised class
$\varrho$	Transmission coefficient of the class of infectious pregnant women
$\zeta$	Transmission coefficient of the class of infectious non-pregnant mothers

### 3. Basic Analysis of the Model

In order to establish the relevance of the disease model (9), we shall perform some basic analyses such as existence of the invariant region and positivity of solutions, disease-free

equilibrium, disease-endemic equilibrium and basic reproduction number.

### 3.1. Invariant Region & Positivity of solutions

Consider the total population  $N$  at time  $t$  is given by

$$N(t) = S_n(t) + I_n(t) + R_n(t) + H(t) + S_p(t) + I_p(t) + R_p(t).$$

We want to establish that the total population is bounded for infinite time  $t$ .

**Theorem 1.** *The set*

$$\Gamma = \left\{ (S_n, I_n, R_n, H, S_p, I_p, R_p) \in \mathbb{R}_+^7 : 0 \leq S_n + I_n + H + R_n + R_p + S_p + I_p = N \leq \frac{\Lambda}{\mu} + \frac{\Pi}{\mu} \right\},$$

*is positively-invariant for the model 9.*

*Proof.* Since the total population  $N$  at time  $t$  is given by

$$\Gamma = \left\{ (S_n, I_n, R_n, H, S_p, I_p, R_p) \in \mathbb{R}_+^7 : 0 \leq S_n + I_n + H + R_n + R_p + S_p + I_p = N \leq \frac{\Lambda}{\mu} + \frac{\Pi}{\mu} \right\}, \tag{10}$$

it follows that

$$\frac{dNt}{dt} = -\varsigma (H + I_n + I_p) + \Lambda + \Pi - \mu Nt \leq \Lambda + \Pi - \mu Nt. \tag{11}$$

$$\therefore \frac{dNt}{dt} + \mu Nt \leq \Lambda + \Pi. \tag{12}$$

$$\therefore Nt \leq ke^{-\mu t} + \frac{\Lambda + \Pi}{\mu}. \tag{13}$$

Taking limit as  $t \rightarrow \infty$ ,

$$N \leq \frac{\Lambda}{\mu} + \frac{\Pi}{\mu} = \frac{\Lambda + \Pi}{\mu}. \tag{14}$$

The inequality 14 which is referred to as the threshold population level shows that if the total women population is greater than the threshold population level, then the total women population reduces asymptotically to the carrying capacity, and if this population is less than the threshold population level, then the solution of the model remains in  $\Gamma$  for all  $t > 0$ . Thus, the region  $\Gamma$  is positively invariant  $\square$

**Theorem 2.** *Suppose*

$$\Gamma = \{ (S_n, I_n, R_n, H, S_p, I_p, R_p) \in \mathbb{R}_+^7 : S_n(0) > 0, I_n(0) > 0, R_n(0) > 0, H(0) > 0, S_p(0) > 0, I_p(0) > 0, R_p(0) > 0 \},$$

*then the solution set*

$$\{ S_n, I_n, R_n, H, S_p, I_p, R_p \},$$

*is positive for all  $t \geq 0$ .*

*Proof.* The first equation of the model is

$$\frac{dS_n}{dt} = \Lambda + \Psi R_n - S_n(\delta + \mu + \chi) + \theta S_p \geq S_n(-(\delta + \mu + \chi)). \tag{15}$$

That is

$$\frac{dS_n}{dt} \geq S_n(-(\delta + \mu + \chi)), \tag{16}$$

$$\ln(\ln)S_n \geq - \int dt(\delta + \mu + \chi). \tag{17}$$

$$\therefore S_n \geq e^{\int(\chi+\delta+\mu)dt}. \tag{18}$$

The constant of integration from the integral is a function of the initial data  $S_n(0)$ . It follows that  $S_n > 0$ . Similarly, we can show that  $I_n(t) > 0, R_n(t) > 0, H(t) > 0, S_p(t) > 0, I_p(t) > 0, R_p(t) > 0$  for all time  $t \geq 0 \square$

### 3.2. Disease-free equilibrium

By setting the right hand side of the model to zero we obtain the following disease-free equilibrium:

$$E_0 = \left( \frac{\theta(\Lambda + \Pi) + \Lambda\mu}{\mu(\delta + \theta + \mu)}, 0, 0, 0, \frac{\delta(\Lambda + \Pi) + \mu\Pi}{\mu(\delta + \theta + \mu)}, 0, 0 \right). \tag{19}$$

### 3.3. Basic reproduction number

The infected classes of the model (1) are  $I_n, H$  and  $I_p$ . We separate the right hand side of the equations of these classes as follows

$$\begin{pmatrix} \chi S_n \\ 0 \\ \beta \chi S_p \end{pmatrix} - \begin{pmatrix} I_n(\delta + \varepsilon + \eta + \mu + \varsigma) - \theta I_p \\ H(\mu + \varsigma + \varphi) - \varepsilon I_n - \alpha I_p \\ I_p(\alpha + \gamma + \theta + \mu + \varsigma) - \delta I_n \end{pmatrix}. \tag{20}$$

Let

$$\mathcal{F} = \begin{pmatrix} \chi S_n \\ 0 \\ \beta \chi S_p \end{pmatrix}, \mathcal{V} = \begin{pmatrix} I_n(\delta + \varepsilon + \eta + \mu + \varsigma) - \theta I_p \\ H(\mu + \varsigma + \varphi) - \varepsilon I_n - \alpha I_p \\ I_p(\alpha + \gamma + \theta + \mu + \varsigma) - \delta I_n \end{pmatrix}. \tag{21}$$

The rows of matrix  $\mathcal{F}$  shows the new infection terms appearing in each infected class of the model, while the rows of matrix  $\mathcal{V}$  shows the transfer terms (old infection terms) also appearing in each infected class of the model. This notation is in line with Driessche and Watmough [19]. This is the next generation matrix approach for finding the basic reproduction number  $R_0$ . The Jacobian of the matrices  $\mathcal{F}$  and  $\mathcal{V}$  at the disease-free equilibrium ( $E_0$ ) are respectively given as

$$F = \begin{pmatrix} -\frac{(k(\varpi-1))(\theta(\Lambda+\Pi)+\Lambda\mu)}{(\Lambda+\Pi)(\delta+\theta+\mu)} & -\frac{(k\iota(\varpi-1))(\theta(\Lambda+\Pi)+\Lambda\mu)}{(\Lambda+\Pi)(\delta+\theta+\mu)} & -\frac{\varrho(k(\varpi-1))(\theta(\Lambda+\Pi)+\Lambda\mu)}{(\Lambda+\Pi)(\delta+\theta+\mu)} \\ 0 & 0 & 0 \\ -\frac{(k\beta(\varpi-1))(\delta(\Lambda+\Pi)+\mu\Pi)}{(\Lambda+\Pi)(\delta+\theta+\mu)} & -\frac{(k\beta\iota(\varpi-1))(\delta(\Lambda+\Pi)+\mu\Pi)}{(\Lambda+\Pi)(\delta+\theta+\mu)} & -\frac{\varrho(k\beta(\varpi-1))(\delta(\Lambda+\Pi)+\mu\Pi)}{(\Lambda+\Pi)(\delta+\theta+\mu)} \end{pmatrix}, \tag{22}$$

$$V = \begin{pmatrix} \delta + \varepsilon + \eta + \mu + \varsigma & 0 & -\theta \\ -\varepsilon & \mu + \varsigma + \varphi & -\alpha \\ -\delta & 0 & \alpha + \gamma + \theta + \mu + \varsigma \end{pmatrix}, \tag{23}$$

$$V^{-1} = \begin{pmatrix} \frac{\alpha + \gamma + \theta + \mu + \varsigma}{(\alpha + \gamma + \theta + \mu + \varsigma)(\delta + \varepsilon + \eta + \mu + \varsigma) - \delta\theta} & 0 & \frac{\theta}{(\alpha + \gamma + \theta + \mu + \varsigma)(\delta + \varepsilon + \eta + \mu + \varsigma) - \delta\theta} \\ \frac{\varepsilon(\alpha + \gamma + \theta + \mu + \varsigma) + \alpha\delta}{(\mu + \varsigma + \varphi)((\alpha + \gamma + \theta + \mu + \varsigma)(\delta + \varepsilon + \eta + \mu + \varsigma) - \delta\theta)} & \frac{1}{\mu + \varsigma + \varphi} & \frac{\alpha(\delta + \varepsilon + \eta + \mu + \varsigma) + \varepsilon\theta}{(\mu + \varsigma + \varphi)((\alpha + \gamma + \theta + \mu + \varsigma)(\delta + \varepsilon + \eta + \mu + \varsigma) - \delta\theta)} \\ \frac{\delta}{(\alpha + \gamma + \theta + \mu + \varsigma)(\delta + \varepsilon + \eta + \mu + \varsigma) - \delta\theta} & 0 & \frac{\delta + \varepsilon + \eta + \mu + \varsigma}{(\alpha + \gamma + \theta + \mu + \varsigma)(\delta + \varepsilon + \eta + \mu + \varsigma) - \delta\theta} \end{pmatrix}, \tag{24}$$

$$FV^{-1} = \begin{pmatrix} a & b & c \\ 0 & 0 & 0 \\ d & e & f \end{pmatrix}, \tag{25}$$

$$\begin{cases} a = \frac{(k(\varpi - 1))(\theta(\Lambda + \Pi) + \Lambda\mu) \left( -\frac{\iota(\varepsilon(\alpha + \gamma + \theta + \mu + \varsigma) + \alpha\delta)}{\mu + \varsigma + \varphi} - \alpha - \gamma - \delta\varrho - \theta - \mu - \varsigma \right)}{(\Lambda + \Pi)(\delta + \theta + \mu)((\alpha + \gamma + \theta + \mu + \varsigma)(\delta + \varepsilon + \eta + \mu + \varsigma) - \delta\theta)}, \\ b = -\frac{(k\iota(\varpi - 1))(\theta(\Lambda + \Pi) + \Lambda\mu)}{(\Lambda + \Pi)(\delta + \theta + \mu)(\mu + \varsigma + \varphi)}, \\ c = \frac{(k(\varpi - 1))(\theta(\Lambda + \Pi) + \Lambda\mu) \left( -\frac{\iota(\alpha(\delta + \varepsilon + \eta + \mu + \varsigma) + \varepsilon\theta)}{\mu + \varsigma + \varphi} - \varrho(\delta + \varepsilon + \eta + \mu + \varsigma) - \theta \right)}{(\Lambda + \Pi)(\delta + \theta + \mu)((\alpha + \gamma + \theta + \mu + \varsigma)(\delta + \varepsilon + \eta + \mu + \varsigma) - \delta\theta)}, \\ d = \frac{(k\beta(\varpi - 1))(\delta(\Lambda + \Pi) + \mu\Pi) \left( -\frac{\iota(\varepsilon(\alpha + \gamma + \theta + \mu + \varsigma) + \alpha\delta)}{\mu + \varsigma + \varphi} - \alpha - \gamma - \delta\varrho - \theta - \mu - \varsigma \right)}{(\Lambda + \Pi)(\delta + \theta + \mu)((\alpha + \gamma + \theta + \mu + \varsigma)(\delta + \varepsilon + \eta + \mu + \varsigma) - \delta\theta)}, \\ e = -\frac{(k\beta\iota(\varpi - 1))(\delta(\Lambda + \Pi) + \mu\Pi)}{(\Lambda + \Pi)(\delta + \theta + \mu)(\mu + \varsigma + \varphi)}, \\ f = \frac{(k\beta(\varpi - 1))(\delta(\Lambda + \Pi) + \mu\Pi) \left( -\frac{\iota(\alpha(\delta + \varepsilon + \eta + \mu + \varsigma) + \varepsilon\theta)}{\mu + \varsigma + \varphi} - \varrho(\delta + \varepsilon + \eta + \mu + \varsigma) - \theta \right)}{(\Lambda + \Pi)(\delta + \theta + \mu)((\alpha + \gamma + \theta + \mu + \varsigma)(\delta + \varepsilon + \eta + \mu + \varsigma) - \delta\theta)}. \end{cases} \tag{26}$$

The spectral radius of the matrix  $FV^{-1}$  is obtained as:

$$\begin{aligned} \rho(FV^{-1}) = & -((k(\varpi - 1))(\alpha((\beta\iota(\Pi(\delta + \mu) + \delta\Lambda))(\delta + \varepsilon + \eta + \mu + \varsigma) + (\Lambda(\theta + \mu) + \theta\Pi) \\ & (\iota(\delta + \varepsilon) + \mu + \varsigma + \varphi)) + \beta\delta^2\Lambda\mu\varrho + \beta\delta^2\Lambda\varrho\varsigma + \beta\delta^2\mu\Pi\varrho + \beta\delta^2\Pi\varrho\varsigma + \varphi((\beta(\Pi(\delta + \mu) + \delta\Lambda)) \\ & (\varrho(\delta + \varepsilon + \eta + \mu + \varsigma) + \theta) + (\delta\varrho + \theta + \mu + \varsigma)(\Lambda(\theta + \mu) + \theta\Pi)) + \beta\mu^3\Pi\varrho + 2\beta\mu^2\Pi\varrho\varsigma \\ & + 2\beta\delta\mu^2\Pi\varrho + \beta\delta\varepsilon\theta\iota\Lambda + \beta\delta\varepsilon\theta\iota\Pi + \beta\delta\varepsilon\Lambda\mu\varrho + \beta\delta\varepsilon\Lambda\varrho\varsigma + \beta\delta\varepsilon\mu\Pi\varrho + \beta\delta\varepsilon\Pi\varrho\varsigma + \beta\delta\eta\Lambda\mu\varrho \\ & + \beta\delta\eta\Lambda\varrho\varsigma + \beta\delta\eta\mu\Pi\varrho + \beta\delta\eta\Pi\varrho\varsigma + \beta\delta\theta\Lambda\mu + \beta\delta\theta\Lambda\varsigma + \beta\delta\theta\mu\Pi + \beta\delta\theta\Pi\varsigma + \beta\delta\Lambda\mu^2\varrho \\ & + 2\beta\delta\Lambda\mu\varrho\varsigma + \beta\delta\Lambda\varrho\varsigma^2 + 3\beta\delta\mu\Pi\varrho\varsigma + \beta\delta\Pi\varrho\varsigma^2 + \beta\varepsilon\mu^2\Pi\varrho + \beta\varepsilon\theta\iota\mu\Pi + \beta\varepsilon\mu\Pi\varrho\varsigma + \beta\eta\mu^2\Pi\varrho \\ & + \beta\eta\mu\Pi\varrho\varsigma + \beta\theta\mu^2\Pi + \beta\theta\mu\Pi\varsigma + \beta\mu\Pi\varrho\varsigma^2 + (\varepsilon\iota + \mu + \varsigma + \varphi)(\gamma(\theta(\Lambda + \Pi) + \Lambda\mu)) \\ & + \delta\theta\Lambda\mu\varrho + \delta\theta\Lambda\varrho\varsigma + \delta\theta\mu\Pi\varrho + \delta\theta\Pi\varrho\varsigma + \delta\Lambda\mu^2\varrho + \delta\Lambda\mu\varrho\varsigma + \varepsilon\theta^2\iota\Lambda + \varepsilon\theta^2\iota\Pi + 2\varepsilon\theta\iota\Lambda\mu \\ & + \varepsilon\theta\iota\Lambda\varsigma + \varepsilon\theta\iota\mu\Pi + \varepsilon\theta\iota\Pi\varsigma + \varepsilon\iota\Lambda\mu^2 + \varepsilon\iota\Lambda\mu\varsigma + \theta^2\Lambda\mu + \theta^2\Lambda\varsigma + \theta^2\mu\Pi + \theta^2\Pi\varsigma + \theta\mu^2\Pi \\ & + 2\theta\Lambda\mu^2 + \theta\Lambda\varsigma^2 + 3\theta\Lambda\mu\varsigma + 2\theta\mu\Pi\varsigma + \theta\Pi\varsigma^2 + \Lambda\mu^3 + 2\Lambda\mu^2\varsigma + \Lambda\mu\varsigma^2)) / \\ & ((\Lambda + \Pi)(\delta + \theta + \mu)(\mu + \varsigma + \varphi)(\alpha(\delta + \varepsilon + \eta + \mu + \varsigma) + \gamma(\delta + \varepsilon + \eta + \mu + \varsigma) + \delta(\mu + \varsigma) \\ & + (\theta + \mu + \varsigma)(\varepsilon + \eta + \mu + \varsigma))). \end{aligned}$$

Substituting the parameter values in table 2 into the spectral radius  $\rho(FV^{-1})$ , we obtain the basic reproduction  $R_0$  as

$$R_0 = \rho(FV^{-1}) = 0.58599. \tag{27}$$

The basic reproduction number represents the average number of secondary cases of the covid-19 infection generated by an infected woman in a completely susceptible women population. If the initial sizes of the compartments of the model are within the basin of attraction of the disease-free equilibrium, then the covid-19 disease can be eliminated from the population when  $R_0 < 1$ . In this case we say that the disease-free equilibrium is locally asymptotically stable if the basic reproduction number is less than one. It is unstable if  $R_0 > 1$ .

Table 2: Parameter Values

Parameters	Value	Source
$\kappa$	1.082	[5]
$\beta$	1.05	Assumed.
$\delta$	0.245	[20]
$\mu$	0.0182	[3]
$p$	0.6	Assumed
$\Lambda$	0.0755	Estimated from [5] and [20]
$\varsigma$	0.022	[3]
$\Psi$	0.00755	Assumed
$\varepsilon$	0.154	citeEnahoroOluwaseunCalistusAbba
$\iota$	0.1	Assumed
$\eta$	1/7 per day	[16]
$\theta$	36.440 births per 1000	[12]
$\varpi$	0.45	Assumed
$\varrho$	0.04	Assumed
$\varphi$	1/14 per day	[16, 22]
$\Pi$	0.0245	Estimated from [5] and [20]
$\sigma$	0.00245	Assumed
$\gamma$	1/7 per day	[16, 22]
$\alpha$	0.154	[5]
$\zeta$	0.07	Assumed

#### 4. Sensitivity Analysis

We want to show the sensitivity of the parameters of the basic reproduction number on the value of  $R_0$ . We employ the approach used by Kizito and Tunwiine [7] to compute the sensitivity of the parameters of  $R_0$ . The sensitivity of a parameter, say  $\mu$ , of  $R_0$  is defined as

$$\zeta_{\mu}^{R_0} = \frac{\partial R_0}{\partial \mu} \times \frac{\mu}{R_0}. \tag{28}$$

The sensitivity analysis of the parameters of the basic reproduction number  $R_0$  reveals the level of sensitivity of each parameter of  $R_0$  to very small changes in their values. This analysis is important because for proper disease control and possible elimination of the covid-19 infection, the sensitivity analysis helps to channel employed control measures to some targeted parameters. If a parameter of  $R_0$  has high positive sensitivity, then any small increment in the value of the parameter can greatly increase the value of  $R_0$  which might cause stability for the disease endemic equilibrium of the the covid-19 infection.

Table 3: Sensitivity of Parameters of  $R_0$ .

Parameters	Value	Sesitivity
$\kappa$	1.082	+1.0000
$\beta$	1.05	+0.6177
$\iota$	0.1	+0.4330
$\theta$	36.440 births per 1000	+0.3075
$\varrho$	0.04	+0.1071
$\alpha$	0.154	+0.0825
$\Lambda$	0.0755	+0.0173
$\Pi$	0.0245	-0.0173
$\mu$	0.0182	-0.0683
$\varepsilon$	0.154	-0.0958
$\eta$	1/7 per day	-0.1477
$\varsigma$	0.022	-0.1491
$\gamma$	1/7 per day	-0.2662
$\varphi$	1/14 per day	-0.2771
$\delta$	0.245	-0.3859
$\varpi$	0.45	-0.8182

The sensitivity indices are shown in Table 3. From the sensitivity analysis, it is seen that the most sensitive parameters of the basic reproduction number,  $R_0$ , are the effective contact rate  $\kappa$  for covid-19 transmission, the modification parameter  $\beta$  accounting for increased susceptibility to covid-19 infection by pregnant women, the transmission coefficient  $\iota$  of the hospitalised class, the rate of delivery  $\theta$  of newborns, the transmission coefficient  $\varrho$  of the infectious pregnant women, and amongst the less sensitive parameters are the conception rate  $\delta$ , the recovery rate  $\varphi$  of hospitalised individuals, the recovery rate  $\gamma$  of infectious pregnant women.

### 5. Bifurcation Analysis

We now examine the type of bifurcation exhibited by the model (9). By this knowledge, we are equipped to know if fixing  $R_0 < 1$  is enough to ‘keep-off’ the disease-endemic equilibrium. The proof is established based on the Centre Manifold Theorem as presented by Castillo-Chavez and Song [2].

**Theorem 3.** [2]: Consider the following general system of ODEs with a parameter  $\phi$ .

$$\frac{dy}{dt} = f(y, \phi), f : \mathbb{R}^n \times \mathbb{R} \text{ and } f \in C^2(\mathbb{R}^n \times \mathbb{R}), \tag{29}$$

where 0 is an equilibrium point of the system (that is,  $f(0, \phi) \equiv 0$  for all  $\phi$  and assume

A1:  $A = D_y f(0, 0) = \left( \frac{\partial f_i}{\partial y_j}(0, 0) \right)$  is the linearization matrix of the system (29) around the equilibrium point 0 with  $\phi$  evaluated at 0. Zero is a simple eigenvalue of A and other eigenvalues of A have negative real parts;

A2: Matrix A has a right eigenvector  $w$  and a left vector  $v$  (each corresponding to the zero eigenvalue).

Let  $f_k$  be the  $k^{th}$  component of  $f$  and

$$a = \sum_{i,j,k=1}^n v_k w_i w_j \frac{\partial^2 f_k}{\partial x_i \partial x_j}(0, 0), \tag{30}$$

$$b = \sum_{i,k=1}^n v_k w_i \frac{\partial^2 f_k}{\partial x_i \partial \phi}(0, 0). \tag{31}$$

The local dynamics of the system (29) around 0 is totally determined by the signs of  $a$  and  $b$ :

1  $a > 0, b > 0$ . When  $\phi < 0$  with  $|\phi| \leq 1$ , 0 is locally asymptotically stable, and there exists a positive unstable equilibrium; when  $0 < \phi \ll 1$ , 0 is unstable and there exists a negative and locally asymptotically stable equilibrium.

2  $a < 0, b < 0$ . When  $\phi < 0$  with  $|\phi| \ll 1$ , 0 is unstable; when  $0 < \phi \ll 1$ , 0 is locally asymptotically stable, and there exists a negative unstable equilibrium.

3  $a > 0, b < 0$ . When  $\phi < 0$  with  $|\phi| \ll 1$ , 0 is unstable, and there exists a locally asymptotically stable negative equilibrium; when  $0 < \phi \ll 1$ , 0 is stable, and a positive unstable equilibrium appears.

4  $a < 0, b > 0$ . When  $\phi$  changes from negative to positive, 0 changes its stability from stable to unstable. Correspondingly, a negative unstable equilibrium becomes positive and locally asymptotically stable.

Particularly, if  $a > 0$  and  $b > 0$ , then a backward bifurcation occurs at  $\phi = 0$ .

*Proof.* We set

$$S_n = x_1, I_n = x_2, R_n = x_3, H = x_4, S_p = x_5, I_p = x_6, R_p = x_7. \tag{32}$$

Thus, the model (9) becomes

$$\begin{cases} \dot{x}_1 = \Lambda - x_1(\delta + \mu + \chi) + \theta x_5 + x_3 \Psi \\ \dot{x}_2 = -x_2(\delta + \varepsilon + \eta + \mu + \varsigma) + \theta x_6 + \chi x_1 \\ \dot{x}_3 = p\varphi x_4 - x_3(\delta + \mu + \Psi) + \eta x_2 + \theta x_7 \\ \dot{x}_4 = \alpha x_6 + \varepsilon x_2 - x_4(\mu + \varsigma + \varphi) \\ \dot{x}_5 = \Pi - x_5(\beta\chi + \theta + \mu) + \delta x_1 + \sigma x_7 \\ \dot{x}_6 = -x_6(\alpha + \gamma + \theta + \mu + \varsigma) + \beta\chi x_5 + \delta x_2 \\ \dot{x}_7 = (1 - p)\varphi x_4 + \gamma x_6 + \delta x_3 - x_7(\theta + \mu + \sigma) \end{cases} \tag{33}$$

Now, the Jacobian of the system (33) evaluated at the disease-free equilibrium ( $E_0$ ), is given by:

$$J_{E_0} = \begin{pmatrix} -\delta - \mu & \frac{(k(\varpi-1)\theta(\Lambda+\Pi)+\Lambda\mu)}{(\Lambda+\Pi)(\delta+\theta+\mu)} & \Psi & \frac{(k\alpha(\varpi-1)\theta(\Lambda+\Pi)+\Lambda\mu)}{(\Lambda+\Pi)(\delta+\theta+\mu)} & \theta & \frac{\theta(k(\varpi-1)\theta(\Lambda+\Pi)+\Lambda\mu)}{(\Lambda+\Pi)(\delta+\theta+\mu)} & 0 \\ 0 & -\delta - \varepsilon - \eta - \frac{(k(\varpi-1)\theta(\Lambda+\Pi)+\Lambda\mu)}{(\Lambda+\Pi)(\delta+\theta+\mu)} - \mu - \varsigma & 0 & -\frac{(k\alpha(\varpi-1)\theta(\Lambda+\Pi)+\Lambda\mu)}{(\Lambda+\Pi)(\delta+\theta+\mu)} & 0 & \theta - \frac{\theta(k(\varpi-1)\theta(\Lambda+\Pi)+\Lambda\mu)}{(\Lambda+\Pi)(\delta+\theta+\mu)} & 0 \\ 0 & \eta & -\delta - \mu - \Psi & p\varphi & 0 & 0 & \theta \\ 0 & \varepsilon & 0 & -\mu - \varsigma - \varphi & 0 & \alpha & 0 \\ \delta & \frac{(k\beta(\varpi-1)(\delta(\Lambda+\Pi)+\mu\Pi))}{(\Lambda+\Pi)(\delta+\theta+\mu)} & 0 & \frac{(k\beta\alpha(\varpi-1)(\delta(\Lambda+\Pi)+\mu\Pi))}{(\Lambda+\Pi)(\delta+\theta+\mu)} & -\theta - \mu & \frac{\theta(k\beta(\varpi-1)(\delta(\Lambda+\Pi)+\mu\Pi))}{(\Lambda+\Pi)(\delta+\theta+\mu)} & \sigma \\ 0 & \delta - \frac{(k\beta(\varpi-1)(\delta(\Lambda+\Pi)+\mu\Pi))}{(\Lambda+\Pi)(\delta+\theta+\mu)} & 0 & -\frac{(k\beta\alpha(\varpi-1)(\delta(\Lambda+\Pi)+\mu\Pi))}{(\Lambda+\Pi)(\delta+\theta+\mu)} & 0 & -\alpha - \gamma - \theta - \frac{\theta(k\beta(\varpi-1)(\delta(\Lambda+\Pi)+\mu\Pi))}{(\Lambda+\Pi)(\delta+\theta+\mu)} - \mu - \varsigma & 0 \\ 0 & 0 & \delta & \varphi - p\varphi & 0 & \gamma & -\theta - \mu - \sigma \end{pmatrix}$$

Let  $\varpi = \varpi^*$  be the bifurcation parameter. We consider the parameter values in table 2 and see that  $\varpi = 1 - 0.9386R_0$ . When  $R_0 = 1$ , we obtain  $\varpi = \varpi^* = 0.06141$ . From the characteristic equation of  $J_{E_0}$  given by  $|J_{E_0} - \lambda I| = 0$ , we obtain the eigenvalues:

$$\begin{cases} \lambda_1 = -0.5978 \\ \lambda_2 = -0.3065 \\ \lambda_3 = -0.2996 \\ \lambda_4 = -0.2638 \\ \lambda_5 = -0.0213 \\ \lambda_6 = -0.0182 \\ \lambda_7 = -1.1001 \times 10^{17} \approx 0. \end{cases} \tag{34}$$

The right eigenvector of  $J(E_0)|_{\varpi=\varpi^*}$  is given by  $(g_1, g_2, g_3, g_4, g_5, g_6, g_7)^T$  where

$$\begin{cases} g_1 = -14.6948g_2, \\ g_2 = g_2 > 0, \\ g_3 = 10.9219g_2, \\ g_4 = 9.41465g_2, \\ g_5 = -98.2523g_2, \\ g_6 = 5.82431g_2, \\ g_7 = 66.1568g_2. \end{cases} \tag{35}$$

The left eigenvector,  $(h_1, h_2, h_3, h_4, h_5, h_6)$ , is also obtained with

$$\begin{cases} h_1 = h_2 = h_5 = 0, h_3 = h_3 > 0, \\ h_4 = 0.403387521843334h_3, \\ h_6 = -0.1809562986293365h_3, \\ h_7 = 0.6382904186372395h_3. \end{cases} \tag{36}$$

From the equations,

$$a = \sum_{i,j,k=1}^n v_k w_i w_j \frac{\partial^2 f_k}{\partial x_i \partial x_j} (S_0, 0, 0, 0), \tag{37}$$

$$b = \sum_{i,k=1}^n v_k w_i \frac{\partial^2 f_k}{\partial x_i \partial \phi} (S_0, 0, 0, 0). \tag{38}$$

we now compute  $a$  and  $b$ . Considering only the non-zero components  $(h_1, h_2, h_3, h_4, h_5, h_6)$  of the left eigenvectors, we obtained:

$$a = 18.823262325556414g_2^2h_3 > 0,$$

$$b = -16.73833317110245g_2h_3 < 0.$$

Since  $a > 0$  and  $b < 0$ , when  $R_0 < 1$ ,  $E_0$  is stable, and there exists a locally asymptotically stable negative disease endemic equilibrium; when  $R_0 > 1$ ,  $E_0$  is unstable, and a positive stable disease endemic equilibrium appears. This is shown in figure 2.

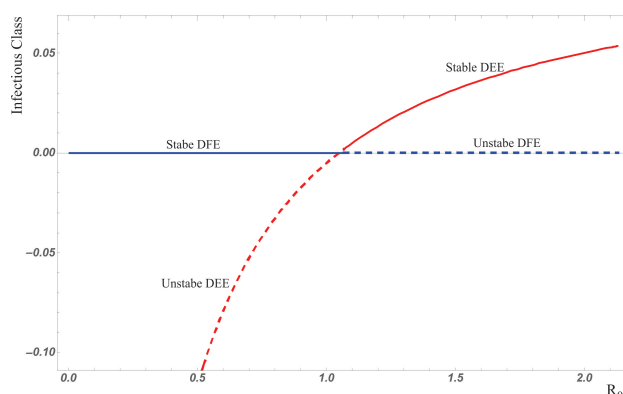


Figure 2: Bifurcation diagram

From the bifurcation plot, it is seen that reducing the value of the basic reproduction number below unity, i.e.  $R_0 < 1$  is enough to minimize the spread of the disease and also eradicate the disease from the population. The parameters pertaining to pregnant women play a major role in controlling the value of the basic reproduction number. From the sensitivity analysis, it can be seen that reducing the values of the effective contact rate  $\kappa$  for covid-19 transmission, the modification parameter  $\beta$  accounting for increased susceptibility to covid-19 infection by pregnant women, Transmission coefficient  $\rho$  of the class

of infectious pregnant women we can successfully achieve  $R_0 < 1$ . Below are simulations showing the effect of the parameters  $\kappa$ ,  $\beta$ ,  $\varrho$ ,  $\theta$ , on the number of infections.

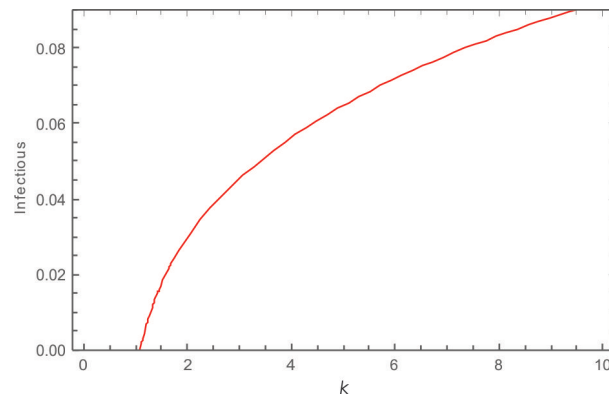


Figure 3: Effect of  $\kappa$  on the infectious class

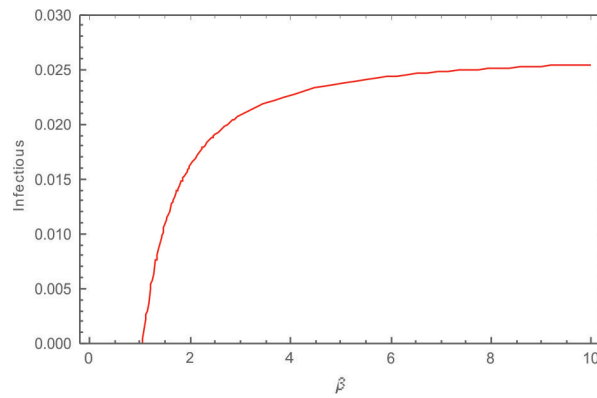


Figure 4: Effect of  $\beta$  on the infectious class

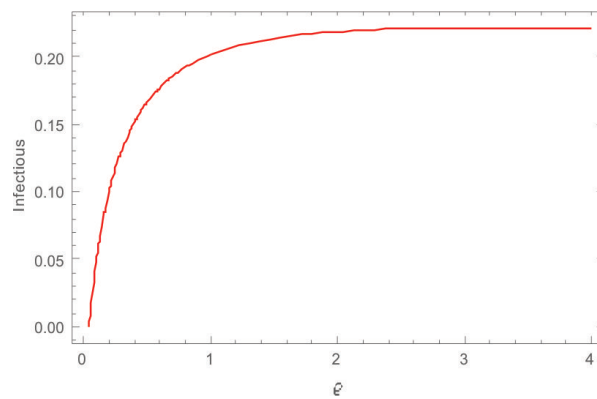
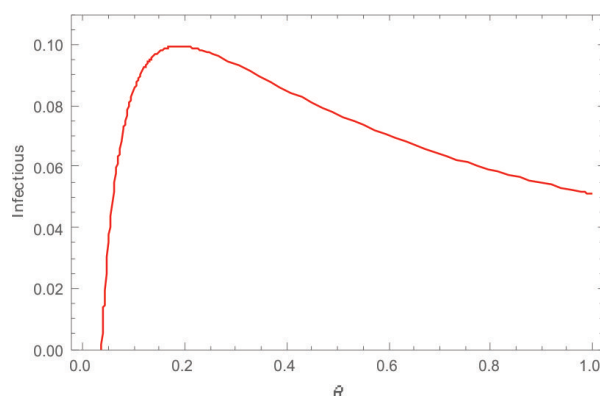


Figure 5: Effect of  $\varrho$  on the infectious class

Figure 6: Effect of  $\theta$  on the infectious class

## 6. Discussion and Conclusion

A deterministic mathematical model is considered in this research paper. The model divides the women population into seven mutually exclusive compartments according to their disease status, namely the pregnant susceptible women  $S_p$ , the non-pregnant susceptible women  $S_n$ , the pregnant infectious women  $I_p$ , the non-pregnant infectious women  $I_n$ , the recovered pregnant women  $R_p$ , the recovered non-pregnant women  $R_n$ , and the hospitalized women  $H$ . The size of each class is a function of time  $t$ . The system of equations is shown in system (9) and the dynamics is clearly displayed in the schematic diagram contained as figure 1. By the basic mathematical analyses, it is revealed that the solution of the system of equations is positive for all time  $t$  and the invariant region  $\Gamma$  was given. The proof which was clearly given also confirmed the existence of the invariant region. The disease-free equilibrium was obtained. The expression for the average number of secondary cases generated by a single infectious individual in an entirely susceptible population, which is given as  $R_0$ , was obtained via the next-generation matrix approach, and the parameter values contained in table 2 resulted in  $R_0 = 0.58599$ . From the sensitivity analysis, it is seen that the most sensitive parameters of the basic reproduction number,  $R_0$ , are  $\kappa$ ,  $\beta$ ,  $\iota$ ,  $\theta$ ,  $\varrho$ , which are the effective contact rate for covid-19 transmission, the modification parameter accounting for increased susceptibility to covid-19 infection by pregnant women, the transmission coefficient of the hospitalised class, the rate of delivery of newborns, and the transmission coefficient of the infectious pregnant women respectively. The less sensitive parameters are the conception rate  $\delta$ , the recovery rate  $\varphi$  of hospitalised individuals, the recovery rate  $\gamma$  of infectious pregnant women. A small increment in the values of the parameters  $\beta$  and  $\varrho$ , causes a great increment in the value of  $R_0$  and hence in the number of infectious cases. Thus, the values of certain parameters of the class of pregnant women affect the number of infectious cases. The bifurcation analysis which was done via the centre manifold theorem revealed a forward bifurcation. That is,  $R_0 < 1$  guarantees the stability of the disease-free equilibrium. This can be achieved by minimizing the most sensitive parameters of the basic reproduction number. The numerical simulations shown in figures 4 – 6 show the effects of the most sensitive parameters of

$R_0$  on the infectious class. We observed that an increase in the values of the parameters causes an increase in the size of the infectious class. From figure 3, we see that setting the effective contact rate  $\kappa > 1.082$ , we obtain a spontaneous increase in the number of infectious cases. Figure 4 revealed that setting  $1.05 < \beta < 4$  shoots up the number of infectious cases. Similarly from figure 5 and 6, setting  $0.04 < \varrho < 1$  and  $0.036 < \theta < 0.1$  also results in shooting up the number of infectious cases. Thus in controlling and eliminating this dreadful enemy of man especially among the women population, these parameters must be properly monitored. The simulations can be employed.

### References

- [1] Baba I., Yusuf A., Nisar K., Abdel-Aty A., Nofal T., "Mathematical model to assess the imposition of Lockdown during COVID-19 pandemic," Results in Physics, Vol. 20, doi:10.1016/j.rinp.2020.103716. 2020.
- [2] Castillo-Chavez C. and Song B., "Dynamical models of tuberculosis and their applications," Mathematical Biosciences and Engineering, vol. 1, pp. 361-404, <https://doi.org/10.3934/mbe.2004.1.361>, 2004.
- [3] Daniel D. O. (2020). Mathematical Model for the Transmission of Covid-19 with Nonlinear Forces of Infection and the Need for Prevention Measure in Nigeria. Journal of Infectious Diseases and Epidemiology, Vol. 6, Doi:10.23937/2474-3658/1510158.
- [4] Dua D. and Samuel B., "Mathematical modeling of COVID-19 infection dynamics in Ghana: Impact evaluation of integrated government and individuals level interventions." Infectious Disease Modelling, Vol. 6, pp. 381-397, <https://doi.org/10.1016/j.idm.2021.01.008>. 2021.
- [5] Enahoro A. I., Oluwaseun S., Calistus N. N., Abba B. G., "Mathematical modeling and analysis of COVID-19 pandemic in Nigeria," Mathematical Biosciences and Engineering, Vol. 17, Issue 6, 7192-7220, doi:<https://doi.org/10.1101/2020.05.22.20110387>, 2020.
- [6] Schwartz D. A., Hyg M. S., Avvad-Portari E., Babal P., et al, "Placenta Tissue Destruction and Insufficiency from COVID-19 Causes Stillbirth and Neonatal Death from Hypoxic-Ischemic Injury: A Study of 68 Cases with SARS-CoV-2 Placentitis from 12 Countries," Archives of Pathology & Laboratory Medicine, <https://doi.org/10.5858/arpa.2022-0029-SA>, 2022.
- [7] Kizito M. and Tumwiine J., "A Mathematical Model of Treatment and Vaccination Interventions of Pneumococcal Pneumonia Infection Dynamics," Journal of Applied Mathematics, Volume 2018, <https://doi.org/10.1155/2018/2539465>, pp 1-15, 2018.
- [8] Kirigia C., "Corona Virus Disease among Pregnant Women: A Systematic Scoping Review," Open Journal of Obstetrics and Gynecology, Vol. 10, No. 5, Doi:10.4236/ojog.2020.1050060, 2020.

- [9] Kotlar B., Gerson E., Petrillo S., et al. "The impact of COVID-19 pandemic on maternal and perinatal health: a scoping review. *Reproductive Health*. Vol. 18, issue 10, <https://doi.org/10.1186/s12978-021-01070-6>, 2021.
- [10] Kumbeni M. T., Apanga P. A., Yeboah E. O., Lettor I. B. K., "Knowledge and preventive practices towards COVID-19 among pregnant women seeking antenatal services in Northern Ghana," *PLoS ONE* 16(6): e0253446. <https://doi.org/10.1371/journal.pone.0253446>, 2021.
- [11] Lee R. W. K., Loy S. L., Yang L., et al., "Attitudes and precaution practices towards COVID-19 among pregnant women in Singapore: a cross-sectional survey," *BMC Pregnancy Childbirth* 20, 675, <https://doi.org/10.1186/s12884-020-03378-w>, 2020.
- [12] Macrotrends (2021). Nigeria Birth Rate 1950 – 2022. <https://www.macrotrends.net/countries/NGA/nigeria/birth-rate>. Accessed January 1st, 2022.
- [13] Macrotrends (2021). Nigeria Death Rate 1950 – 2022. <https://www.macrotrends.net/countries/NGA/nigeria/death-rate>. Accessed January 1st, 2022.
- [14] Macrotrends (2021). Nigeria Fertility Rate 1950 – 2021. <https://www.macrotrends.net/countries/NGA/nigeria/fertility-rate>. Accessed January 1st, 2022.
- [15] Ndairou F., Area I., Nieto J. and Torres D. F. M. (2020), "Mathematical Modeling of COVID-19 Transmission Dynamics with a Case Study of Wuhan," *Chaos, Solitons and Fractals*, Vol. 135, 10.1016/j.chaos.2020.109846, 2020.
- [16] Tang B., Wang X., Li Q., Bragazzi N. L., Tang S., Xiao Y., et al, "Estimation of transmission risk of the 2019-nCoV and its implication for public health interventions," *Journal of Clinical Medicine*, doi:10.2139/ssrn.3525558, 2020.
- [17] Panahi L., Amiri M., Pouy S., "Risks of Novel Coronavirus Disease (COVID-19) in Pregnancy; a Narrative Review," *Archives of academic emergency medicine*, Vol. 8, doi:10.22037/aaem.v8i1.595, 2020.
- [18] Parisa S., Zahra A., Maryam G., Roghayem A., "The severity of COVID-19 among pregnant women and the risk of averse maternal outcomes," *International Journal of Gynecology & Obstetrics*. Vol. 154, Issue 1, pp. 92-99. <https://doi.org/10.1002/ijgo.13700>. 2021.
- [19] Van den Driessche P. and Watmough J., "Reproduction Numbers and Sub-Threshold Endemic Equilibria for Compartmental Models of Disease Transmission," *Mathematical Biosciences*, vol. 180, pp. 29-48, [https://doi.org/10.1016/S0025-5564\(02\)00108-6](https://doi.org/10.1016/S0025-5564(02)00108-6), 2002.

- [20] van Eekelen R., Tjon-Kon-Fat R., Bossuyt P. M. M., van Geloven N., Eijkemans M. J. C., Bendsorp A. J., van der Veen F., Mol B. W., van Wely M., "National conception rates in couples with unexplained or mild male subfertility scheduled for fertility treatment: a secondary analysis of a randomized controlled trial," *Human Reproduction*, Vol. 33, Issue 5, <https://doi.org/10.1093/humrep/dey051>, 2018.
- [21] Wendy, N. P., Olise, P. K., "Is Pregnancy a risk factor of COVID-19?" *European Journal of Obstetrics & Gynecology and Reproduction Biology*, Vol. 252, pp. 605 – 609, DOI:<https://doi.org/10.1016/j.ejogrb.2020.06.058>, 2020.
- [22] Zhou F., Yu T., Du R., Fan G., Liu Y., Liu Z., et al., "Clinical course and risk factors for mortality of adult inpatients with COVID-19 in Wuhan, China: a retrospective cohort study," *The lancet*, Vol. 395, doi:10.1016/S0140-6736(20)30566-3, 2020.
- [23] Shaher M., Omar A. A., Banan M., "Piecewise optimal fractional reproducing kernel solution and convergence analysis for the Atangana-Baleanu-Caputo model of the Lienard's equation", *Fractals*, Vol. 28, doi:10.1142/S0218348X20400071, 2020.
- [24] Momani S., Maayah B., and Omar A. A., "The reproducing Kernel Algorithm for numerical solution of Van Der Pol Damping Model in view of the Atangana–Baleanu Fractional approach", *Fractals*, Vol. 28, No. 08, <https://doi.org/10.1142/S0218348X20400101>, 2020.
- [25] Omar A. A., "Computational algorithm for solving singular Fredholm time-fractional partial integrodifferential equations with error estimates," *Journal of Applied Mathematics and Computing*, Vol. 59, doi:10.1007/s12190-018-1176-x, 2019.
- [26] Omar A. A., Hasan R., "The RKHS method for numerical treatment for integrodifferential algebraic systems of temporal two-point BVPs," *Neural Computing and Applications*, Vol 30, doi:10.1007/s00521-017-2845-7, 2018.